



ATLAS Note

GROUP-2017-XX

30th December 2018



Draft version 0.1

Electron-to-photon fake rate measurement

Yifan Hu^{a,b}, Yanping Huang^a, Shuo Han^{a,b}, Kurt Brendlinger^b

^aIHEP,CAS

^bDESY

A measurement of electron-to-photon fake rate using 79.9 fb^{-1} of pp collisions collected by the ATLAS detector in 2015, 2016 and 2017 is presented. The $e \rightarrow \gamma$ fake rate, a fraction of $Z \rightarrow e^+e^-$ events is reconstructed as $Z \rightarrow e\gamma$ can be estimated from Z to 2 body decays due to the misidentification. An excess of the $e\gamma$ final state with an invariant mass close to Z -mass is a clear symptom to be observed in the data, and compared to the simulation results.

12 **Contents**

13	1 Introduction	3
14	2 Data and MC samples	3
15	3 Event Selection	5
16	3.1 Classification of cluster reconstruction in ambiguity tool	5
17	3.2 Event selection	5
18	3.3 Object selection	5
19	4 Fake rate measurement	6
20	4.1 Fit method investigation	7
21	4.1.1 Original Tag-And-Probe normalization method	7
22	4.1.2 Background Tempalte validation	8
23	4.2 Fit strategis validation	9
24	4.2.1 Only $W\gamma$ background pdf + $Z \rightarrow ee$ MC signal	10
25	4.2.2 Author 16 template background pdf + $Z \rightarrow ee$ MC signal	10
26	4.2.3 $W\gamma$ and author 16 template background pdf + $Z \rightarrow ee$ MC signal	10
27	4.2.4 Fit results comparison between different strategies	10
28	5 Systematic Uncertainties	25
29	6 Results	25
30	7 Conclusion	25
31	Appendices	28
32	A Fit results performance	28

33 1 Introduction

34 Electrons and photons leave a very similar signature in the detector. Although photons reconstruction
 35 algorithms are designed to reduce this mis-identification of electrons as photons, in order to keep the
 36 photon and electron reconstruction efficiency as high as possible, a strict overlap removal is not enforced.
 37 In case of doubt, the same electromagnetic clusters, generated by the same particle, is reconstructed under
 38 both the electron and the photon hypothesis. This implies that genuine electrons may end up reconstructed
 39 as photons. If the reconstructed objects generated by a real electron passing the analysis offline selection
 40 for photons, they will make up the so called electron-to-photon misidentification background, so electron-
 41 to-photon fake rate measurement has been designed.

42 This note presents a measurement of the electron-to-photon fake rate using the full pp collision dataset
 43 collected by the ATLAS detector in 2015,2016 and 2017,corresponding to an integrated luminosity of
 44 79.9 fb^{-1} .

45 We definite the electron-to-photon fake rate using reconstructed clusters from genuine electron assuming
 46 electron reconstruction efficiency and scale factor are very close to 1 :

$$F_{e \rightarrow \gamma} = \frac{N_{reco-\gamma}}{N_{\text{geniue electrons}}}$$

47 Where the $N_{reco-\gamma}$ is the number of reconstructed photon originating from a true electron particle,
 48 $N_{\text{geniue electrons}}$ is the number of true electron particle. The fake rate is determined from the number of
 49 dielectron candidates from $Z \rightarrow ee$ decays that are either reconstructed as ee or $e\gamma$. Such yields are
 50 estimated from the ee and $e\gamma$ invariant mass spectra observed in the data, looking in those spectra for
 51 a peak near the Z boson mass and subtracting the yields of background candidates obtained from the
 52 background fit.

53 The note is organised as follows. Section 2 lists the data and simulation samples used for the measurement.
 54 Section 3 introduce the data and MC samples we used. The event selection is described in Section 4
 55 and the criteria that define a γ_{reco} and an e_{reco} are given there. Section 5 illustrates the method used
 56 to measure the fakerate in data, and the associated sources of systematic uncertainties are discussed in
 57 Section 6. Section 7 gives the final results and is followedby a short conclusion.

58 2 Data and MC samples

59 The full 2015,2016 and 2017 pp collision data is used in this study.

60 Events must belong to the luminosity blocks specified in the good runs lists below:

- 61 1. data15_13TeV.periodAllYear_DetStatus-v89-pro21-02_Unknown_PHYS_StandardGRL_All_Good_25ns.xml
- 62 2. data16_13TeV.periodAllYear_DetStatus-v89-pro21-01_DQDefects-00-02-04_PHYS_StandardGRL_All_Good_25ns.xml
- 63 3. data17_13TeV.periodAllYear_DetStatus-v97-pro21-13_Unknown_PHYS_StandardGRL_All_Good_25ns_Triggerno17e33prim.xml

64 respectively for the data collected in 2015,2016 or 2017.

65 Events were collected using the following triggers for 2015/2016/2017 data:

66 1. 2015:

- 67 a) HLT_e24_lhmedium_L1EM18VH
- 68 b) HLT_e24_lhmedium_L1EM20VH
- 69 c) HLT_e60_lhmedium
- 70 d) HLT_e120_lhloose

71 2. 2016:

- 72 a) HLT_e26_lhtight_nod0_ivarloose
- 73 b) HLT_e60_lhmedium_nod0
- 74 c) HLT_e60_medium
- 75 d) HLT_e140_lhloose_nod0
- 76 e) HLT_e300_etcut

77 3. 2017:

- 78 a) HLT•nderscore e26_lhtight_nod0_ivarloose
- 79 b) HLT_e60_lhmedium_nod0
- 80 c) HLT_e140_lhloose_nod0
- 81 d) HLT_e300_etcut

82 The corresponding integrated luminosity is 3.2fb^{-1} for 2015, 32.9fb^{-1} for 2016 and 43.8fb^{-1} for 2017.

83 The Monte Carlo (MC) simulation events used in this analysis are generated with POWHEG [1], a Next-
 84 to-Leading order event generator, interfaced with PYTHIA8 [2], which takes care of the description of
 85 the parton showering and underlying event. All the simulated samples include the effects of multiple
 86 pp interactions in the same and neighbouring bunch crossings (pile-up) and were processed through the
 87 ATLAS detector simulation [3] based on Geant4 [4]. All samples are produced using the ATLAS-R2-
 88 2015-03-01 detector geometry simulation tag. The MC events were finally reconstructed with the same
 89 algorithms used for the data.

90 The MC datasets we use is : $Z \rightarrow ee$

- 91 • 2015+2016: mc16_13TeV.361106.PowhegPythia8EvtGen_AZNLOCTEQ6L1_Zee.deriv.DAOD_EGAM1.e3601_s3126_r9364_r9315_p3374
- 92 • 2017: mc16_13TeV.361106.PowhegPythia8EvtGen_AZNLOCTEQ6L1_Zee.deriv.DAOD_EGAM1.e3601_s3126_r10201_r10210_p3374

93 Data and MC simulations are under the same reconstruction release (Athena version 21). For the
 94 analysis we used EGAM1 derived DAODs centrally produced from the AODs for the reconstruction. The
 95 DAODs with ptag p3372 for data and ptag p3374 for MC, are all corresponding to version of 21.2.8.0
 96 AtlasDerivation.

97 You can find some text snippets that can be used in papers in `template/atlas-snippets.tex`. Some
 98 of the snippets need the `jetetmiss` option passed to `atlasphysics`.

⁹⁹ 3 Event Selection

¹⁰⁰ We add the criteria on the objects and events to confirm that we get exactly what we want. Considering
¹⁰¹ that we base our cuts on the ambiguous tool, there is a need to introduce it firstly.

¹⁰² 3.1 Classification of cluster reconstruction in ambiguity tool

¹⁰³ Based on the reconstruction and classifications for an energy cluster in the calorimeter: electrons, photons,
¹⁰⁴ ambiguous. The ambiguous type includes all the particles that are not enough well reconstructed to be
¹⁰⁵ tagged clearly as photon or an electron. More accurately:

¹⁰⁶ • *photons*: A candidate particle is tagged as a photon if there are no tracks with at least four hits in the
¹⁰⁷ silicon detector matched to the calorimeter cluster, or if a double silicon conversion vertex is found and
¹⁰⁸ the electron track is part of the vertex and it has no hits in the pixel detector.

¹⁰⁹ • *electrons*: A candidate particle is tagged as an electron if no conversion vertex is matched with its
¹¹⁰ track and the track is reconstructed with at least two hits in the pixel detector and four hits in the silicon
¹¹¹ detector. In the case a vertex is matched the particle can still be tagged as electron if the vertex is not
¹¹² a double-silicon tracks vertex, or, if this is the case, only one track matched to the vertex has innermost
¹¹³ pixel hits.

¹¹⁴ • *ambiguous*: A candidate particle is tagged as an ambiguous if the cluster is matched with a track that
¹¹⁵ fails the quality cuts and that has no hits in the pixel detector. In this case the object is reconstructed as
¹¹⁶ both an electron and a photon.

¹¹⁷ 3.2 Event selection

¹¹⁸ Use Tag-and-probe selection method for Z->ee/e γ :

- ¹¹⁹ • At least 1e+1e/ γ
- ¹²⁰ • Zmass window: promise from z->ee process
- ¹²¹ • Vertex cut (vertex number ≥ 1), EventCleaning cut, GRL, single electron trigger

¹²² 3.3 Object selection

- ¹²³ • Tag and probe objects:
 - ¹²⁴ – author cut(electron: author=1||author=16;photons: author=1);
 - ¹²⁵ – fiducial cuts(tag and probe outside of η crack(1.37 1.52) but tag inside 2.47 and probe inside
¹²⁶ 2.37);
 - ¹²⁷ – Pt cut(tag $\geq 25\text{GeV}$,probe $\geq 5\text{GeV}$);
 - ¹²⁸ – OQ cut;
 - ¹²⁹ – Jet veto: isolated from AntKt4 jet with $E_t > 20 \text{ GeV}$ within $\Delta R = 0.4$.

Not reviewed, for internal circulation only

- 130 • Tag electrons: Tight electron ID; Trigger match.
- 131 • Probe electrons:
 - 132 – Denominator cut
 - 133 * Opposite-charge with tag electron
 - 134 * Track quality: 7 silicon hit and 1 pixel hit
 - 135 * truth match to Z for MC (and electron originated from Z at truth level)
 - 136 – Numerator cut
 - 137 * Ambiguous cut(just author =16)
 - 138 * match with a reco-photon which has the most proximal pt with the probe electron in $\Delta R < 0.2$
 - 140 • probe γ
 - 141 – Denominator cut
 - 142 * e- γ overlap removal: remove the photon when the $dR(e,\gamma) < 0.15$
 - 143 * truth match for photons: can match with an electron form Z boson($dR(e,y)2 < 0.04$) at truth level
 - 145 * photon author=4
 - 146 – Numerator cut: same as Denominator

147 4 Fake rate measurement

148 Based on the ambiguous tool introduced before, the fake rate measured here is closed related to the
 149 ambiguous type. It's obtained from the ratio:

$$F_{e \rightarrow \gamma} = \frac{N_{\text{ambiguouselectron}} + N_{\text{photons(author=4)}}}{N_{\text{electrons+photons(author=4)}}}$$

150 The selected electrons and photons are filled in each η or p_T bin. For the η bins, we divide into 14
 151 bins: $\pm(0.0-0.6-0.8-1.15-1.37)$ and $\pm(1.52-1.81-2.01-2.37)$; for the p_T bins , they are divided into 9 bins:
 152 25-35-45-55-65-75-90-120-180-300GeV. And then fit on $m_{ee/e\gamma}$ peak in 14 η bins(9 p_T bins) to get the
 153 numerator and denominator.

Not reviewed, for internal circulation only

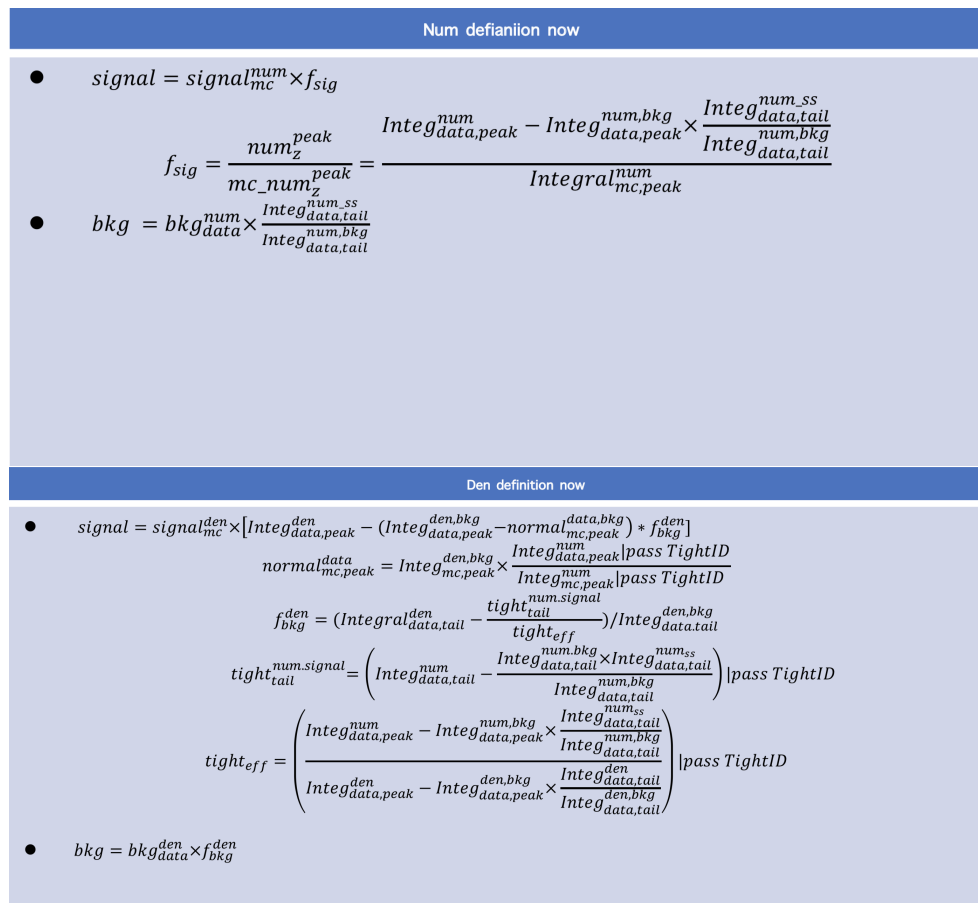


Figure 1: Normalization factor in Tag-And-Probe package.

154 **4.1 Fit method investigation**

155 **4.1.1 Original Tag-And-Probe normalization method**

156 Aim for the fit method, basically under the Tag-And-Probe package, the fit plot are normalized by the
 157 factor calculated via the tail and the peak region integral events and tight efficiency, which is expected to
 158 ??? (figure1):

159 With using the basical background template cut and traditional normalization method :

- 160 • Author 1||16 electron
- 161 • Pass track quality but fail >=2 shower shapes (Rhad, Reta, Weta, Wstot, Eratio, DeltaEta)
- 162 • invert isolation cut(etcone40/pt>0.05)

163 In this case, the numerator conclude the ambiguous electrons(author cut=16) and author=4 photons, the
 164 denominator conclude electrons(author cut=1) components more),so the fit plots are shown in figure2:

165 We can see clearly that the numerator fit need to be improved, the discrepancy between the data and MC is
 166 too large. The denominator seems not too bad. As to clarify which part is the main reason to account for

¹⁶⁷ the bad fit, we remove the authot=4 photons part to see if it can be fitted well only containing the electrons
¹⁶⁸ part(ambiguous electrons and real electrons), the fit plots show in figure3.

¹⁶⁹ The fit has been much improved by removing the */gamma* part, that is to say, the author=4 photons part
¹⁷⁰ of the fit should be the main reason for the bad fit. Therefore, we only reserve the photons part in the
¹⁷¹ numerator to see how the fit changes(firure4):

¹⁷² The plots get much worse than the original fit plots or the plots without the photon part.

¹⁷³ 4.1.2 Background Tempalte validation

¹⁷⁴ So we have good reason to believe that the suitability of the fit are related to different components,eg.
¹⁷⁵ different author cuts. Moreover, treat different components using different fit method is a must. To better
¹⁷⁶ understand the case, I compare the MC signal shape and data shape under each kind of author cuts:
¹⁷⁷ ambiguous electrons-author cut=16;only photons-author cut=4;both-author cut=16||4.(figure5)

¹⁷⁸ From the comparision, MC signal shape in tails doesn't change much when use different author cut but
¹⁷⁹ numerator data shape (contains Signal+Background) changes a lot under author cut=4 (only reco photons).

¹⁸⁰ Thus, the background template shape (which uses author=1||16) may not describe the Z mass spectrum
¹⁸¹ under author=4 cut well.

¹⁸² In this case, we define the different background templates for the different components to be fitted better:

- ¹⁸³ • Author=1||16 template(nominal case)

- ¹⁸⁴ • Author=16 template (“templ16”): same as nominal case, but without author=1 electrons

- ¹⁸⁵ • Author=4 template: Add the cut below in Z->ee data and subtract the MC leakage in the data photon
¹⁸⁶ bkg template:

- ¹⁸⁷ – Test1: Inverse ID (LoosePrime5)(figure6)

- ¹⁸⁸ – Test2: Inverse ID (LoosePrime5) and Isolation cut topoetcone40/pt>0.05(figure7)

- ¹⁸⁹ – Test3: Inverse ID (LoosePrime5) and Isolation cut topoetcone20/pt>0.065 and ptcone20/pt>0.05(figure8)

¹⁹⁰

- ¹⁹¹ – Test4: Inverse ID (LoosePrime5) and Isolation cut topoetcone20/pt>0.2 and ptcone20/pt>0.2(figure9)

¹⁹²

¹⁹³ We test 4 kinds of the cut for the background template. With the cut getting stronger, the template looks
¹⁹⁴ more like the real photon part background. However, there seems a peak at 90GeV point. So we consider
¹⁹⁵ getting the background template with subtrating the signal leakage in photon(author=4) template control
¹⁹⁶ region(figure10,11):

- ¹⁹⁷ • Normalize the MC shape according the cross section

- ¹⁹⁸ • add the photon background template cut on MC sample to get the signal leakage

- ¹⁹⁹ • Subtract the MC leakage in the data photon background template

200 From figure11, we can see that some difference can be seen on the author = 16 and author = 4 control
 201 shapes, that may account for different process, which is need to be investigated more. Besides that, the
 202 statistic in data is too low to extract a background shape for author = 4 case. So we need use $W\gamma$ samples
 203 to understand the background shape of Zee tag-and-probe selection at truth level.

204 Therefore, we use the $W\gamma$ sample (AthDerivation 21.2.34.0) of MC16a and MC16d, corresponding
 205 to the data15/16 and data17 and divided to 5 slices to pass the numerator signal cut (except for the
 206 truth match) and get the $W\gamma$ shape, which represents the photon components in the background. By
 207 the comparison between the $W\gamma$ shape and author=16 template(figure12), we find they shows a little
 208 difference. By checking the $W\gamma$ contamination in the author=16 template, we also find it's little enough
 209 to be ignored(1/10000 to 1/100000) as figure13 shows. Finally, we decide to use the $W\gamma$ template for a
 210 template variationi.

211 Apart from the photon components, electron compoents,eg. Wj background are represented by author =
 212 16 template. With investigating more, we find the Z->ee leakage(MC Z->ee sample pass the Template 16
 213 cut) should be considered. Because the leakage give much contribution in the author = 16 template(more
 214 than 1/10) as figure14 shows. Nevertheless, we see that there is an apparent dip when subtracting the leakage,
 215 which is inappropriate for the background analysis and will cause the over-subtraction.

216 To correctly subtract the Z->ee leakage, we have to find a method to get a smooth template but not the
 217 author=16 template with subtracting the leakage directly(figure15). Assuming that the leakage mainly
 218 distribute around [60GeV,120GeV], then we can get a formular like this:

$$\frac{\int_{60}^{250} \text{Zeeleakage}}{\int_{60}^{250} \text{Template16}} \approx \frac{\int_{60}^{120} \text{Zeeleakage}}{\int_{60}^{120} \text{Template16}} = \frac{Nsig_{60}^{120}}{Nbkg_{60}^{120}}$$

219 For the $Nsig_{60}^{120}$ and $Nsig_{60}^{120}$, we fit the Template16 using the Bern4+Z->ee leakage(figure16), $Nsig_{60}^{120}$
 220 comes from the Zee leakage shape in the fit and integral at [60,120], $Nsig_{60}^{120}$
 221 comes from Bern4 pdf shape in the fit and integral at [60,120]. Finally, we normalize the Z->ee leakage
 222 shape to the factor:

$$f = \frac{\int_{60}^{120} \text{Template16} \times Nsig_{60}^{120}}{Nsig_{60}^{120} + Nbkg_{60}^{120}}$$

223 to avoid the over-subtraction.

224 Finally, we got the modified author=16 template with the modified Z->ee leakage subtraction and compare
 225 them with the template16 before.(figure17)

226 4.2 Fit strategis validation

227 As to get the fake rate results by calculating the integral in the Z->ee peak range[80GeV,100GeV],
 228 precise two leptons mass spectrum(ee or e/gamma)fit results matters a lot.we fix the shape from the
 229 data background and Monto Carlo signal: create the background pdf and signal pdf separately using
 230 background template histograms and Z->ee Mont Carlo histograms. And then fit the data using the
 231 background and signal pdf with floating the normalization factor.

232 4.2.1 Only $W\gamma$ background pdf + $Z \rightarrow ee$ MC signal

233 As mentioned in the subsection 4.1, $W\gamma$ shape represent the photon background component. Through
234 this strategy, we find truth photons should give non-negligible contribution in the numerator background
235 and the bump at low mass range for numerator disappears.(figure18)

236 4.2.2 Author 16 template background pdf + $Z \rightarrow ee$ MC signal

237 Author 16 template represent $wj+jj$ background components, so we consider three kinds of case here:
238 without leakage subtraction(figure19), with original leakage subtraction(figure20) and modified $Z \rightarrow ee$
239 leakage subtraction(fugure21). We find that discrepancy at low mass range for numerator still appear a
240 little.

241 4.2.3 $W\gamma$ and author 16 template background pdf + $Z \rightarrow ee$ MC signal

242 Similar to the strategy 2, there are still three kinds of cases: $W\gamma$ +author 16 template without $Z \rightarrow ee$
243 leakage subtraction(figure22), $W\gamma$ +author 16 template with origianl $Z \rightarrow ee$ leakage subtraction(figure23),
244 $W\gamma$ + author 16 template with modified $Z \rightarrow ee$ leakage subtraction(figure24). As imagined, this Strategy
245 gives the best fit result for we add another degree of freedom and discrepancy at low mass range for
246 numerator is better than before.

247 4.2.4 Fit results comparison between different strategies

248 The difference are not too much between these strategies. But still we can find the signal leakage over-
249 subtraction cause more influence in the barrel region. Besides that, appropriate signal leakage subtraction
250 may lead to a “balanced fit” and is better than trusting the MC out-of-the-box.(figure25)

Not reviewed, for internal circulation only

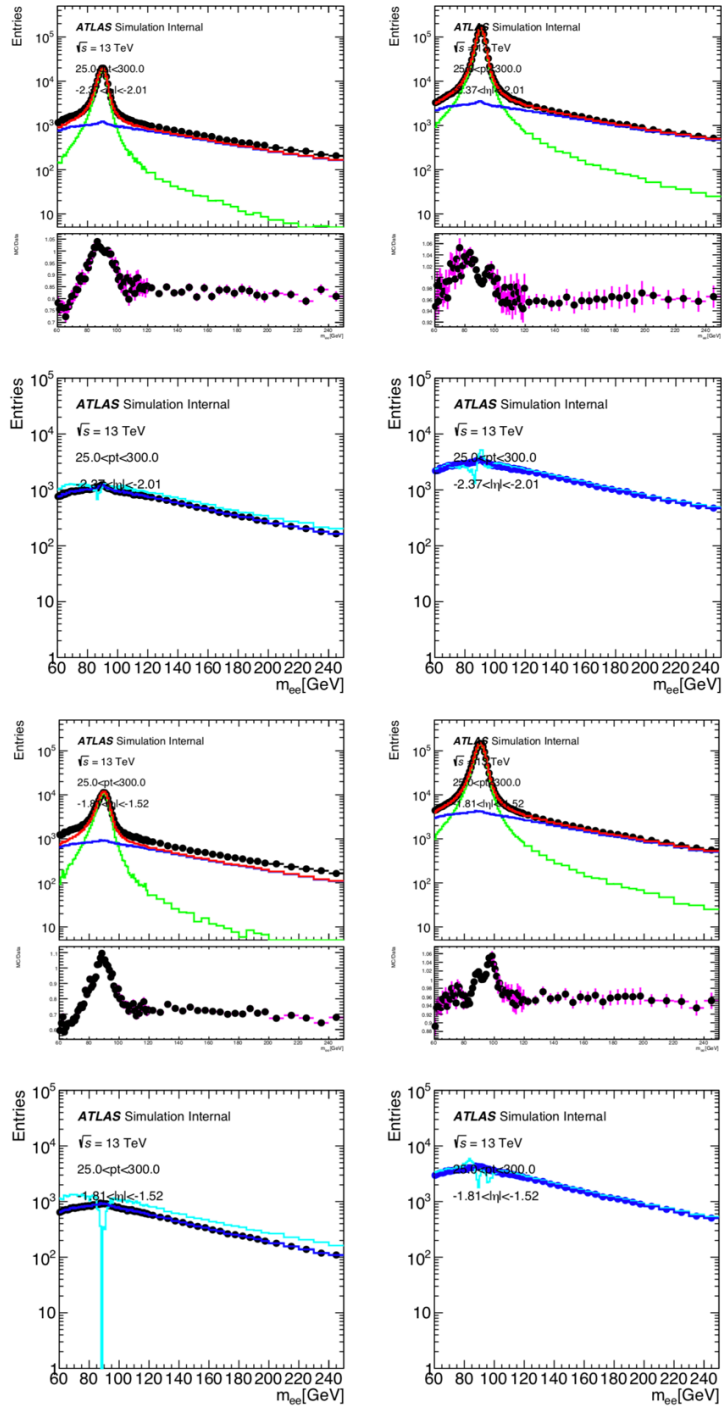


Figure 2: m_{ee}/ϵ_y fit plots using the normalization factor of Tag-And-Probe package, the left plots show the numerator performance and the right plots show the denominator performance.

Not reviewed, for internal circulation only

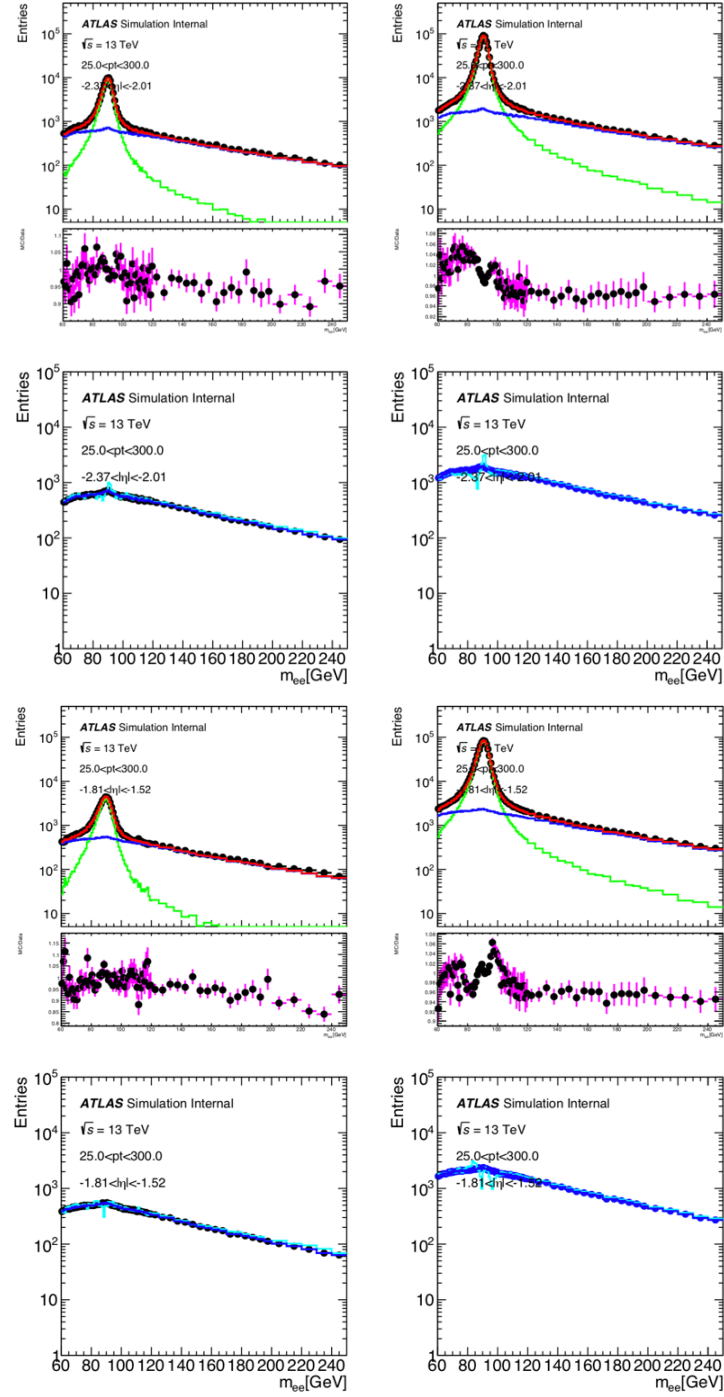


Figure 3: m_{ee} fit plots using the normalization factor of Tag-And-Probe package but removing the authot=4 photons part in both numerator(the left plots) and denominator(the right plots).

Not reviewed, for internal circulation only

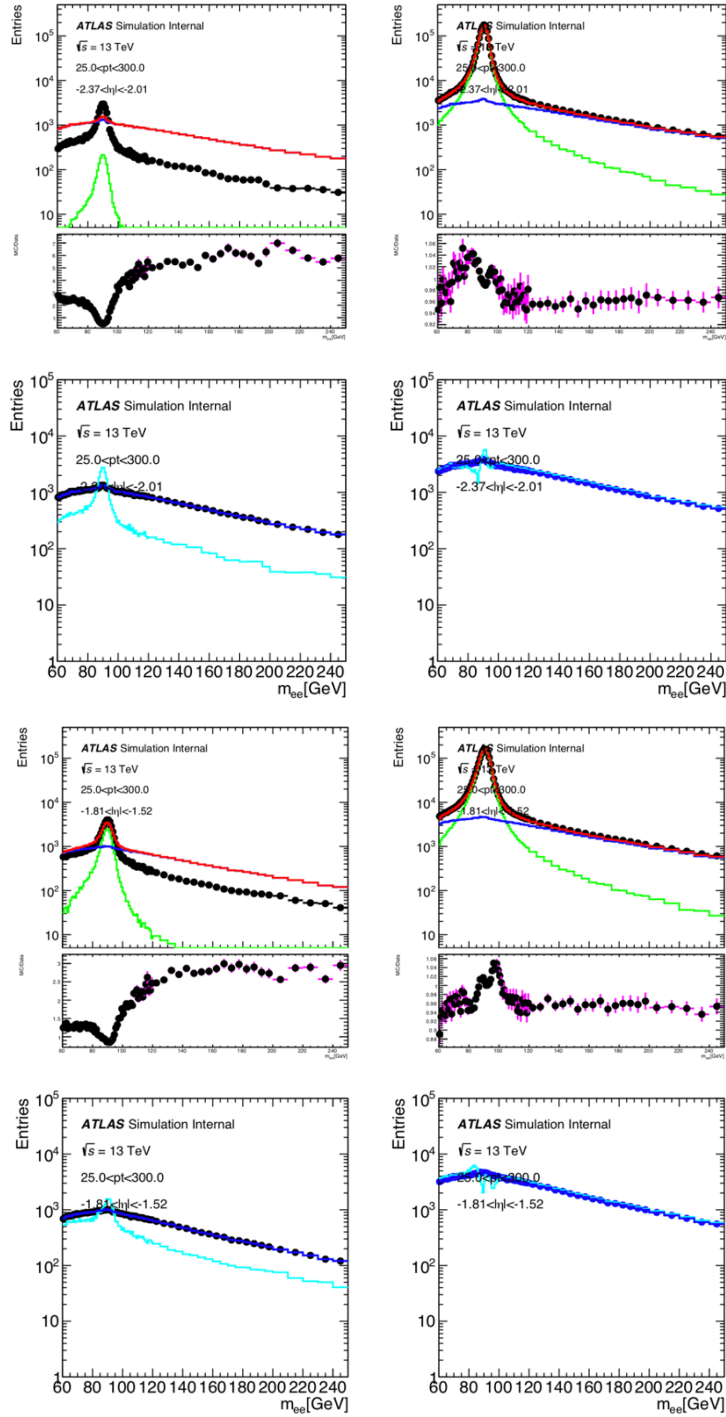


Figure 4: $m_{e\gamma}$ fit plots only reserving the authot=4 photons part for the numerator as the left plots show and $m_{ee}/m_{e\gamma}$ fit plots for the denominator as right plots show with both using the normalization factor of Tag-And-Probe package.

Not reviewed, for internal circulation only

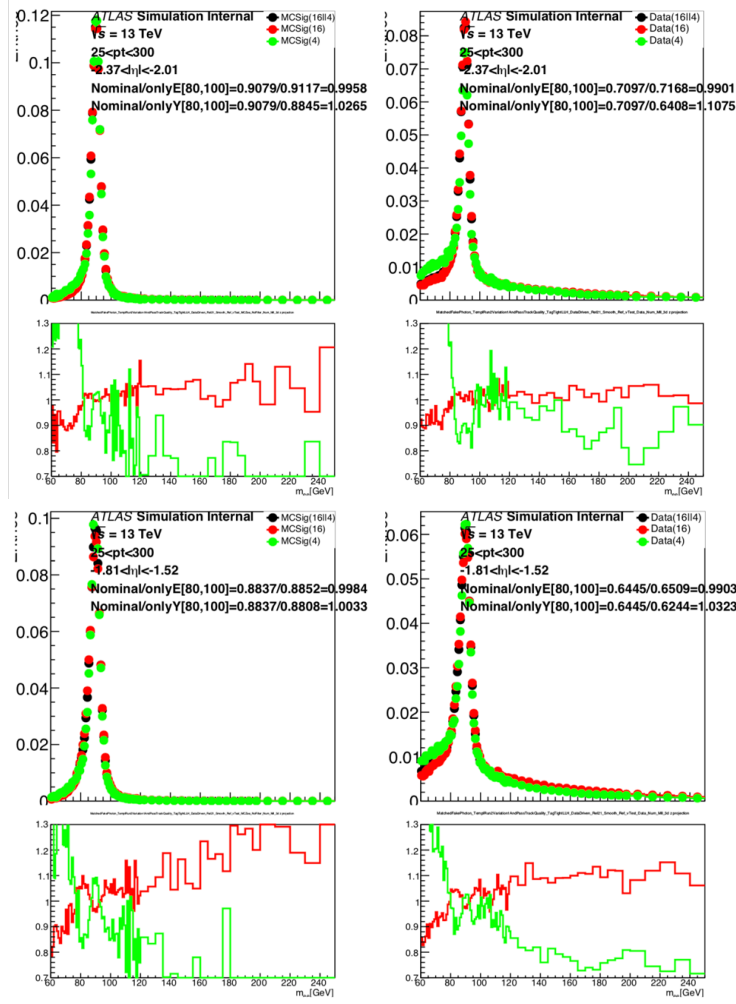


Figure 5: MC signal shape comparison(left plots) and data shape comparison(right plots) under different author cuts: ambiguous electrons-author cut=16;only photons-author cut=4;both-author cut=16||4. The formula on the plots show the ratio of the nominal case(author=4||16) events(integral between [80GeV,100GeV]region) and the one photon(or only ambiguous) part case events.

Not reviewed, for internal circulation only

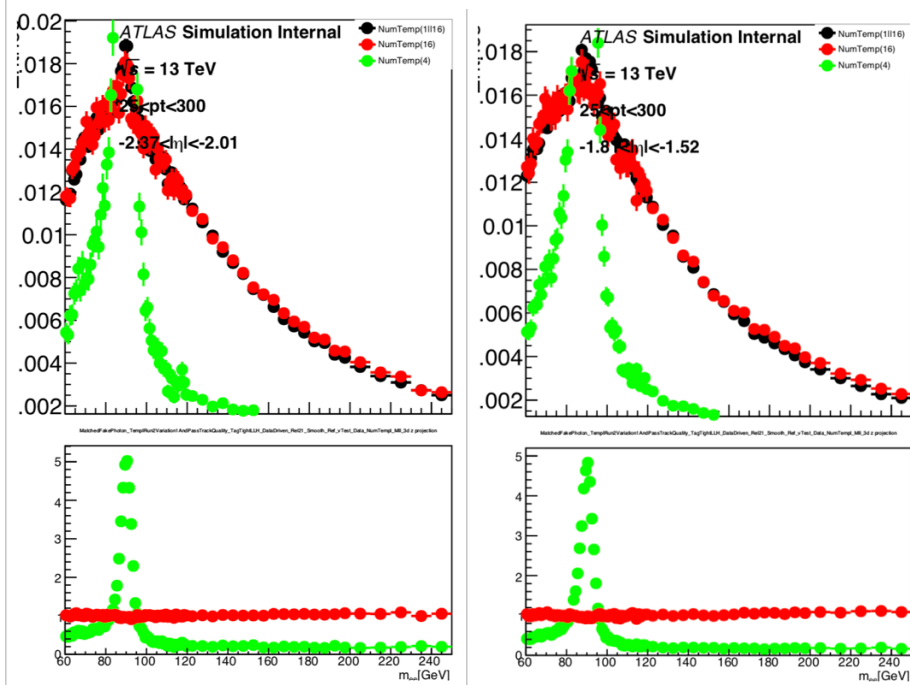


Figure 6: photons part background template with LoosPrime5 cut in η region $[-2.37, -2.01]$ and $[-1.81, -1.52]$.

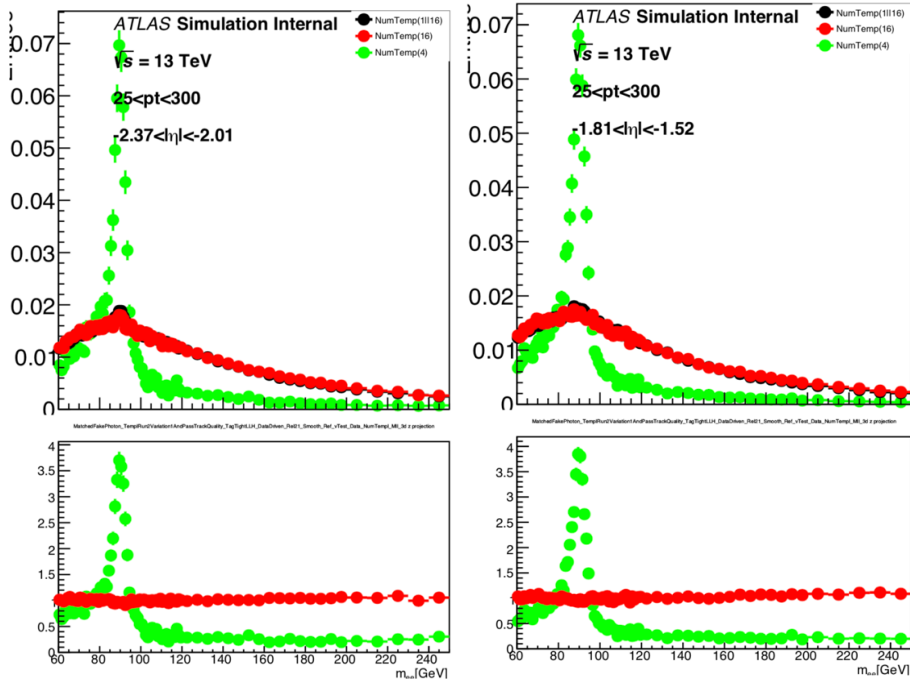


Figure 7: photons part background template with LoosPrime5 and topoetcone40/ $\text{pt} > 0.05$ cut in η region $[-2.37, -2.01]$ and $[-1.81, -1.52]$.

Not reviewed, for internal circulation only

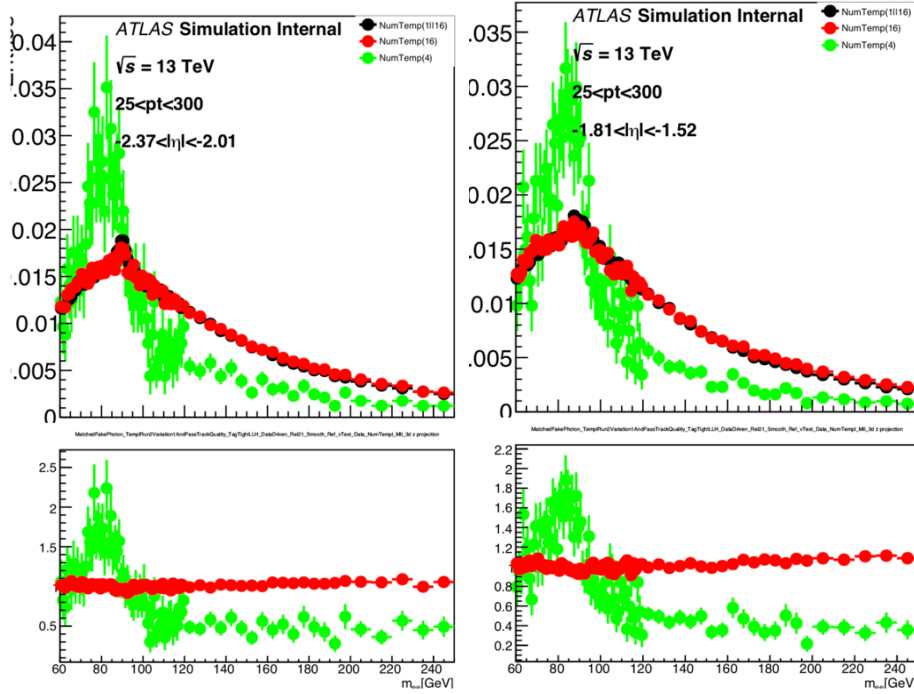


Figure 8: photons part background template with LoosPrime5 and topoetcone20/pt>0.065 and ptcone20/pt>0.05 isolation cut in η region[-2.37,-2.01] and [-1.81,-1.52].

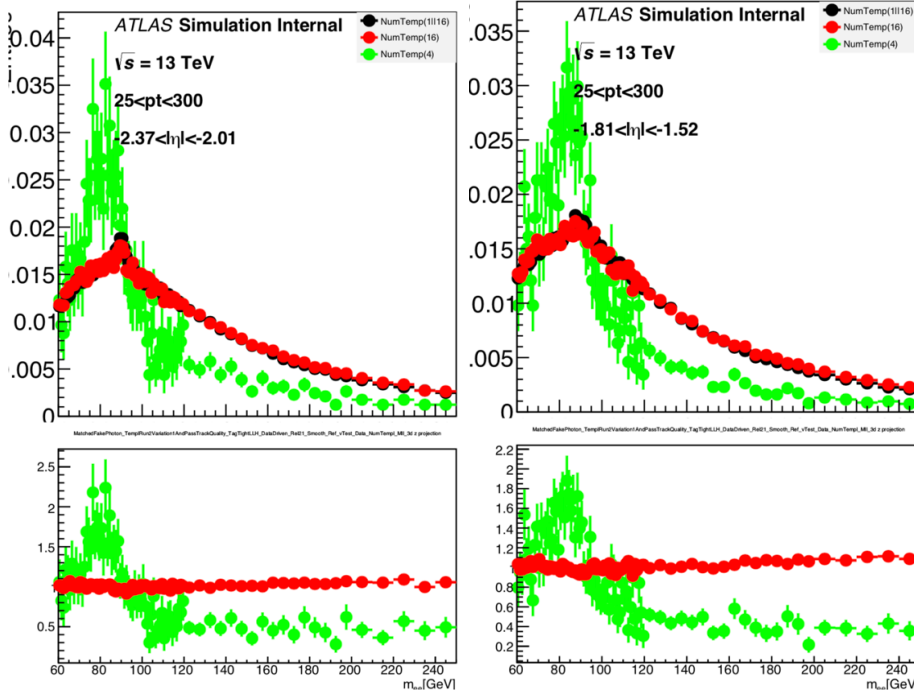


Figure 9: photons part background template with LoosPrime5 and topoetcone20/pt>0.2 and ptcone20/pt>0.2 isolation cut in η region[-2.37,-2.01] and [-1.81,-1.52].

Not reviewed, for internal circulation only

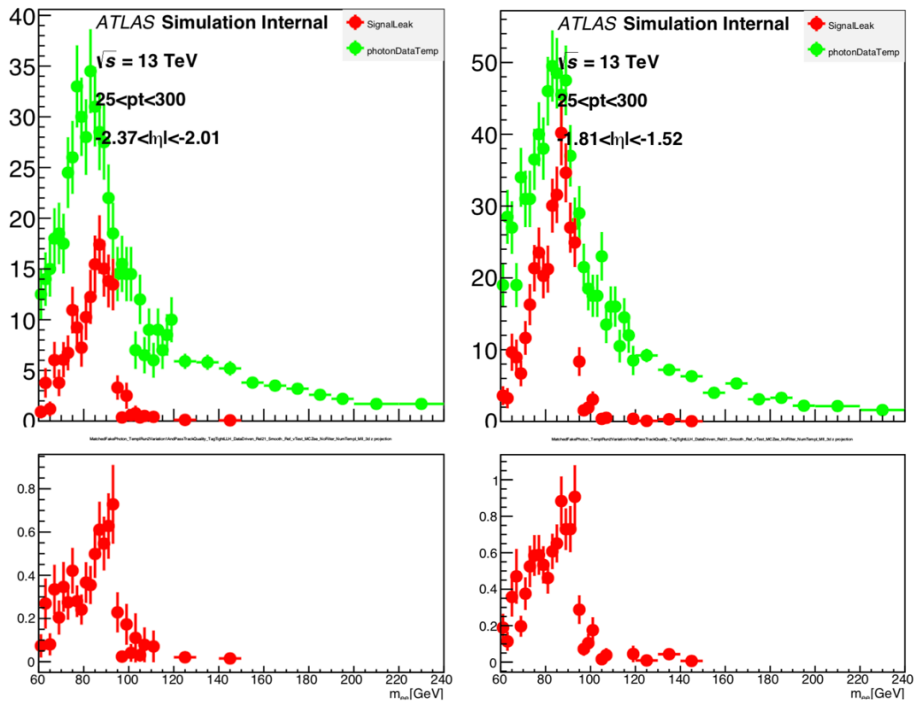


Figure 10: Comparison between the Z signal leakage in MC and only photon data template. Red line represents the signal leakage and the green line represents the photon background template.

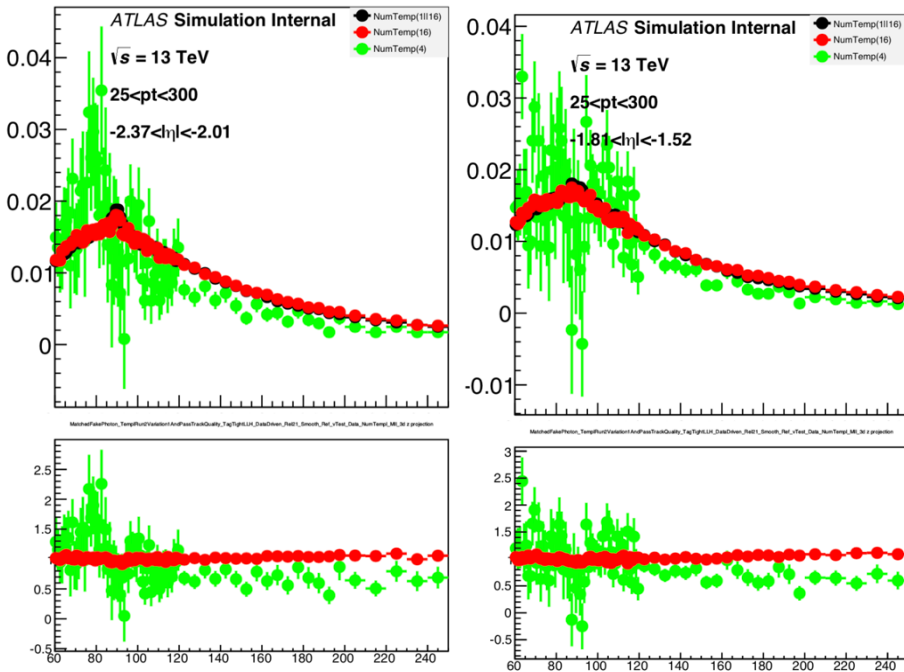


Figure 11: Photon background template after subtracting the Zee leakage

Not reviewed, for internal circulation only

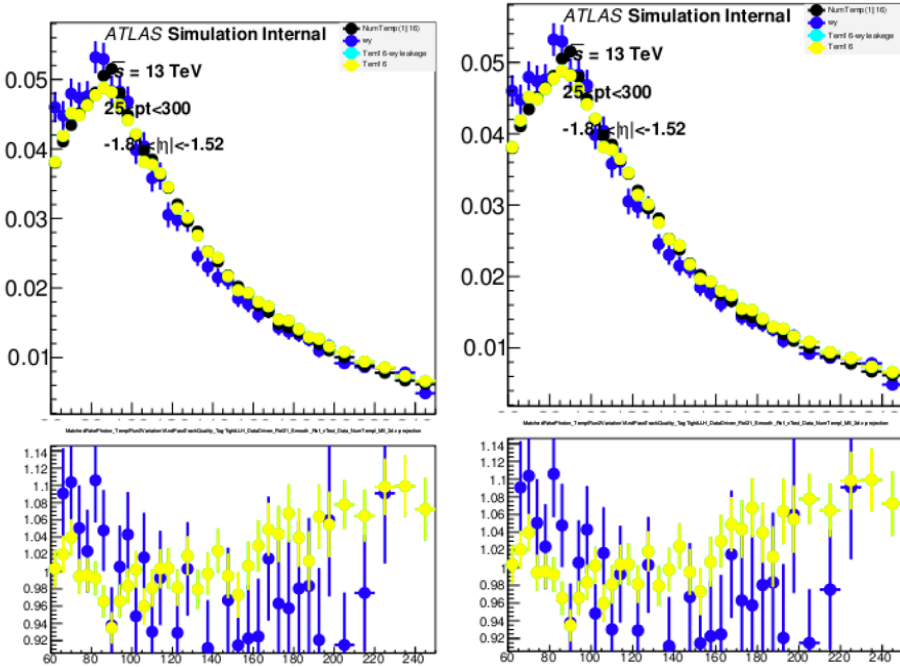


Figure 12: Comparison between the $W\gamma$ shape and author=16 template for η region $[-2.37, -1.81]$ and $[-1.81, -1.52]$.

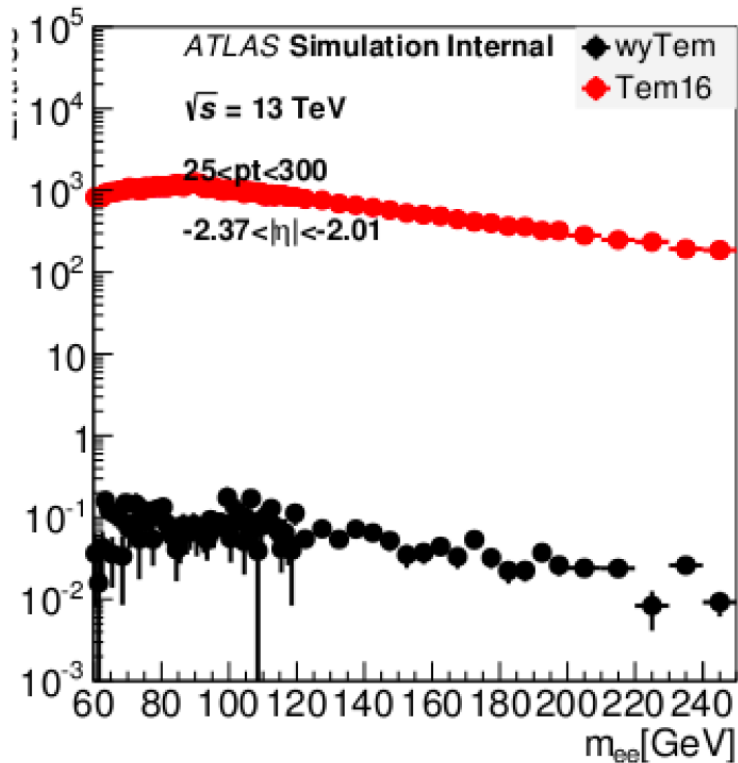


Figure 13: Check the $W\gamma$ contamination in the author=16 template. It's about 1/10000 to 1/100000 in the template.

Not reviewed, for internal circulation only

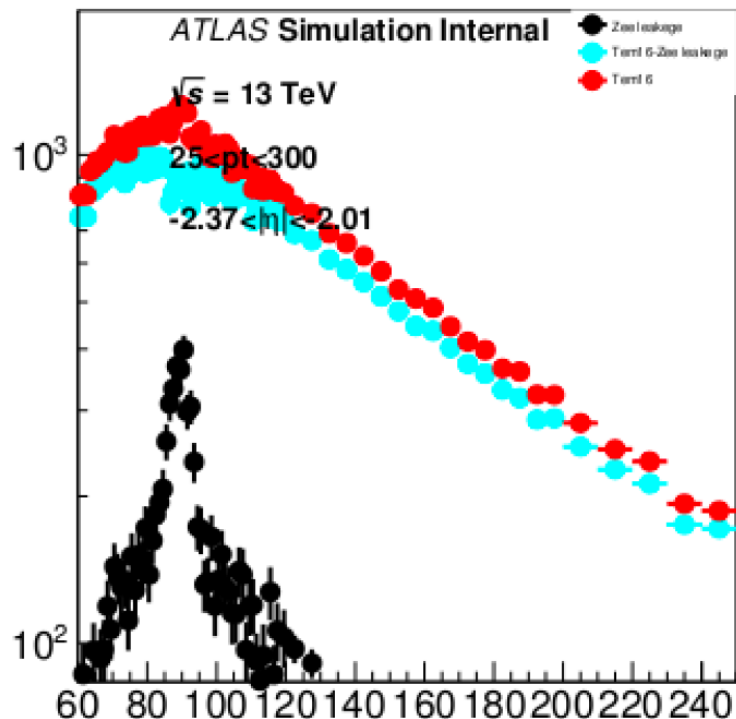


Figure 14: Check the $Z \rightarrow ee$ leakage contamination in the author=16 template. It's more than 1/10 in the template. And if we subtract the signal leakage in the template 16, it will cause a dip, which may cause from the over-subtraction for the template 16.

Not reviewed, for internal circulation only

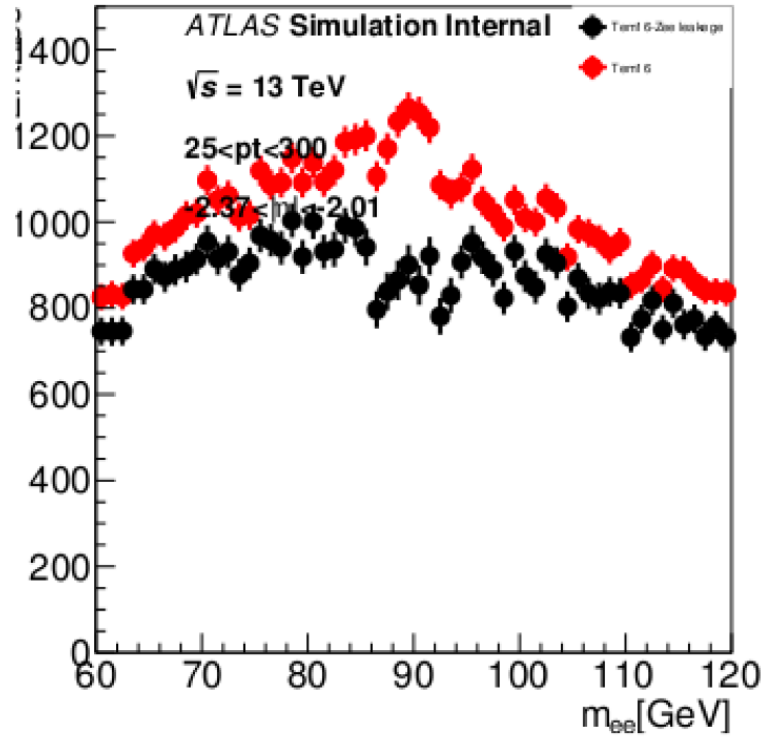


Figure 15: Big Difference between the template16 with and without the Zee leakage.

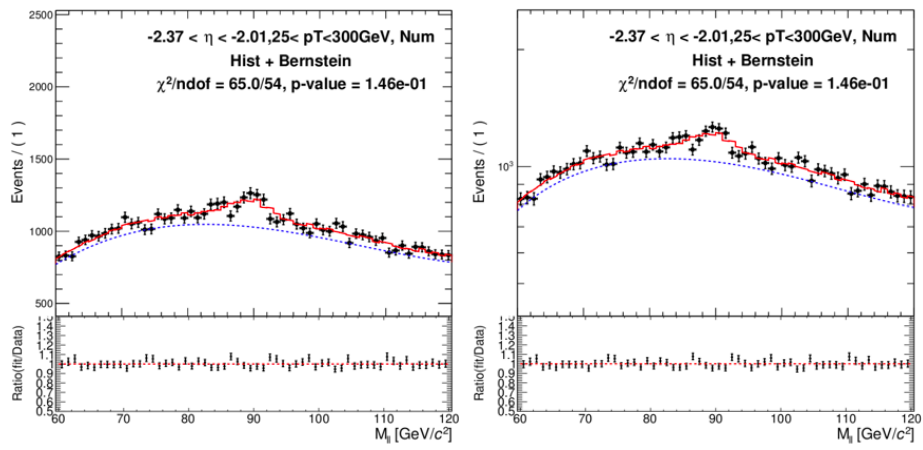


Figure 16: Fit the Template16 using the Bern4+Z->ee leakage. Left plot shows the normal scale and right plot shows the log scale. In which we fit it well for the accurate leakage subtraction.

Not reviewed, for internal circulation only

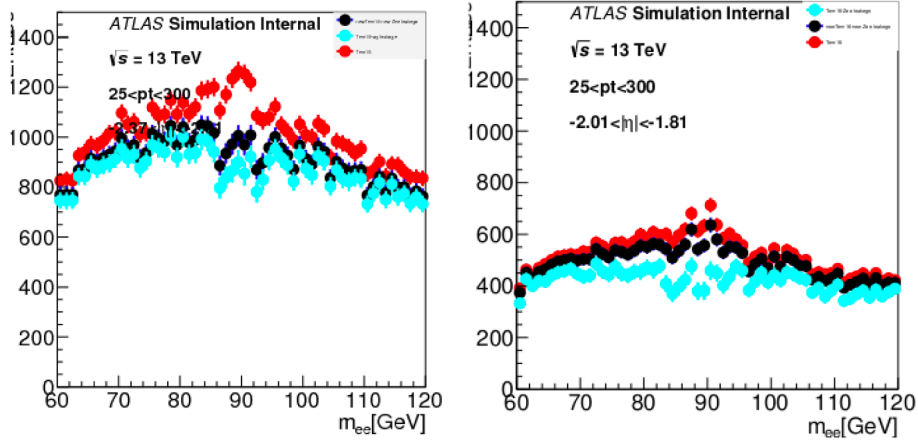


Figure 17: Comparison between the author=16 template, template16 with original $Z \rightarrow ee$ leakage subtraction and modified leakage subtraction. The dip has been disappeared after the modification.

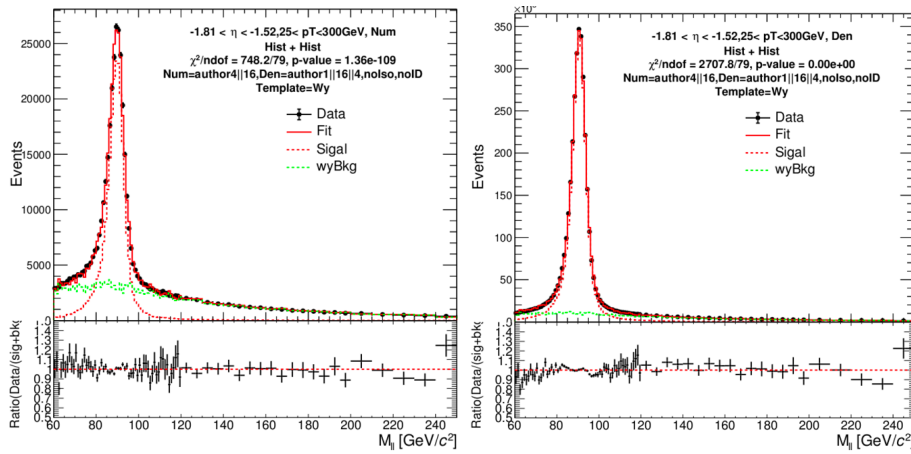


Figure 18: Truth photon should give non-negligible contribution in numerator background and the bump at low mass range for numerator disappears but the denominator shows new discrepancy.

Not reviewed, for internal circulation only

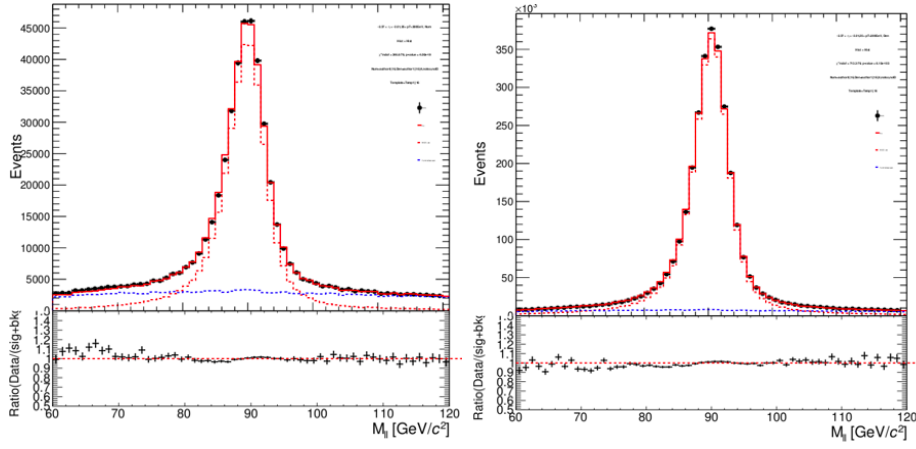


Figure 19: Author 16 template without $Z \rightarrow ee$ leakage subtraction as background pdf

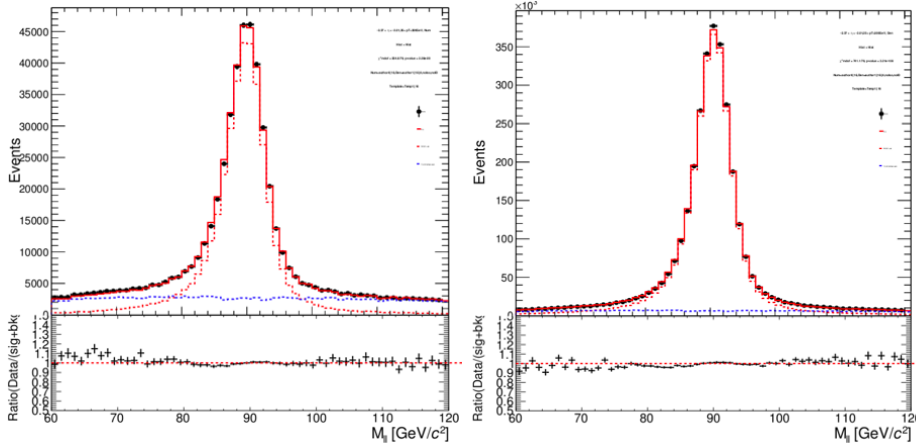


Figure 20: Author 16 template with original $Z \rightarrow ee$ leakage subtraction as background pdf

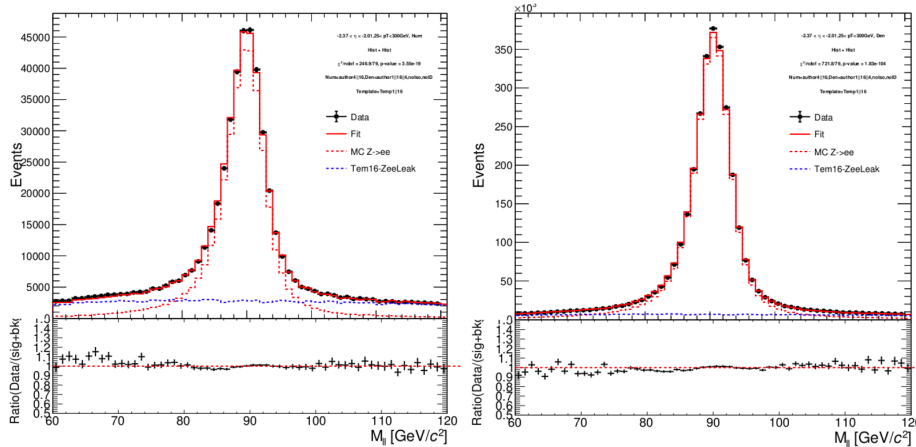


Figure 21: Author 16 template with modified $Z \rightarrow ee$ leakage subtraction as background pdf

Not reviewed, for internal circulation only

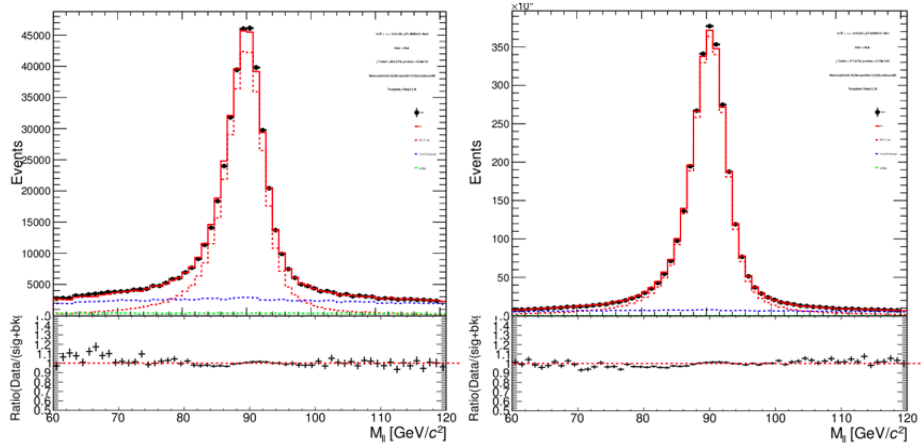


Figure 22: $W\gamma$ and author 16 template without $Z \rightarrow ee$ leakage subtraction as background pdf

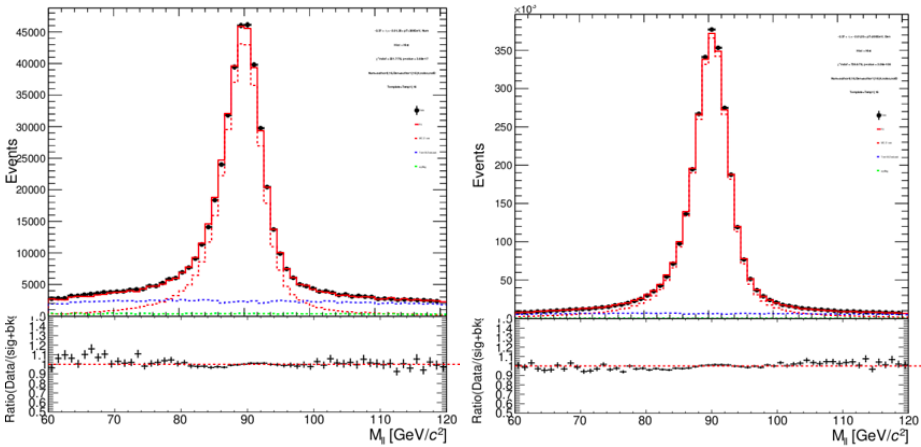


Figure 23: $W\gamma$ and author 16 template with original $Z \rightarrow ee$ leakage subtraction as background pdf

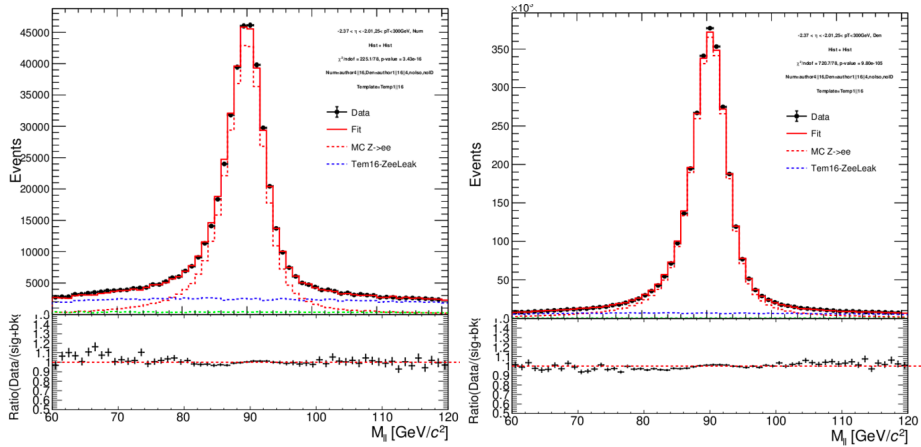


Figure 24: $W\gamma$ and author 16 template with modified $Z \rightarrow ee$ leakage subtraction as background pdf

Not reviewed, for internal circulation only

Strategy	Eta region	Signal events Chi2/Ndof		Fake Rate
		Num	Den	
1 Wy	[-2.37,-2.01]	1.42e+05 1271.2/79	1.13e+06 3164.5/79	12.58%
	[-1.81,-1.52]	9.09e+04 748.2/79	1.23e+06. 2707.8/79	7.41%
	[-2.37,-2.01]	1.42e+05 246.6/79	1.13e+06. 713.3/79	12.54%
2 Temp16 w/o Zee leak subtr.	[-1.81,-1.52]	9.33e+04. 723.0/79	1.24e+06. 1163.3/79	7.54%
	[-2.37,-2.01]	1.45e+05 254.8/79	1.14e+06 741.1/79	12.71%
Template16 w/ Zee subtr.	[-1.81,-1.52]	9.60e+04 896.1/79	1.25e+06. 1700.7/79	7.70%
	[-2.37,-2.01]	1.44e+05 246.9/79	1.14e+06 721.8/79	12.66%
3 Mix wy + temp16 w/o Zee subtr.	[-1.81,-1.52]	9.33e+04 723.0/79	1.24e+06 1163.4/79	7.54%
	[-2.37,-2.01]	1.42e+05 223.3/78	1.13e+06. 711.1/78	12.54%
	[-1.81,-1.52]	9.20e+04 483.3/78	1.23e+06. 1052.0/78	7.45%
Mix wy + temp16 w/Zee subtr.	[-2.37,-2.01]	1.44e+05 231.7/78	1.14e+06 739.6/78	12.68%
	[-1.81,-1.52]	9.30e+04. 523.5/78	1.24e+06 1364.2/78	7.50%
Mix wy+temp16 w/update zee subtr.	[-2.37,-2.01]	1.44e+05 225.1/78	1.14e+06 720.7/78	12.64%
	[-1.81,-1.52]	9.20e+04. 483.3/78	1.23e+06 1052.1/78	7.45%

Figure 25: Fit results comparison between different strategies.

251 **5 Systematic Uncertainties**

252 **6 Results**

253 The fake rate result measured using the 2015 and 2016 data is compared with the value of the fake rate
 254 obtained from the $Z \rightarrow ee$ Monte Carlo sample. The differences between the evaluations obtained from
 255 data and from simulated events are described by the ratio that allow us to mimic the observation behaviour
 256 in data from the simulation.

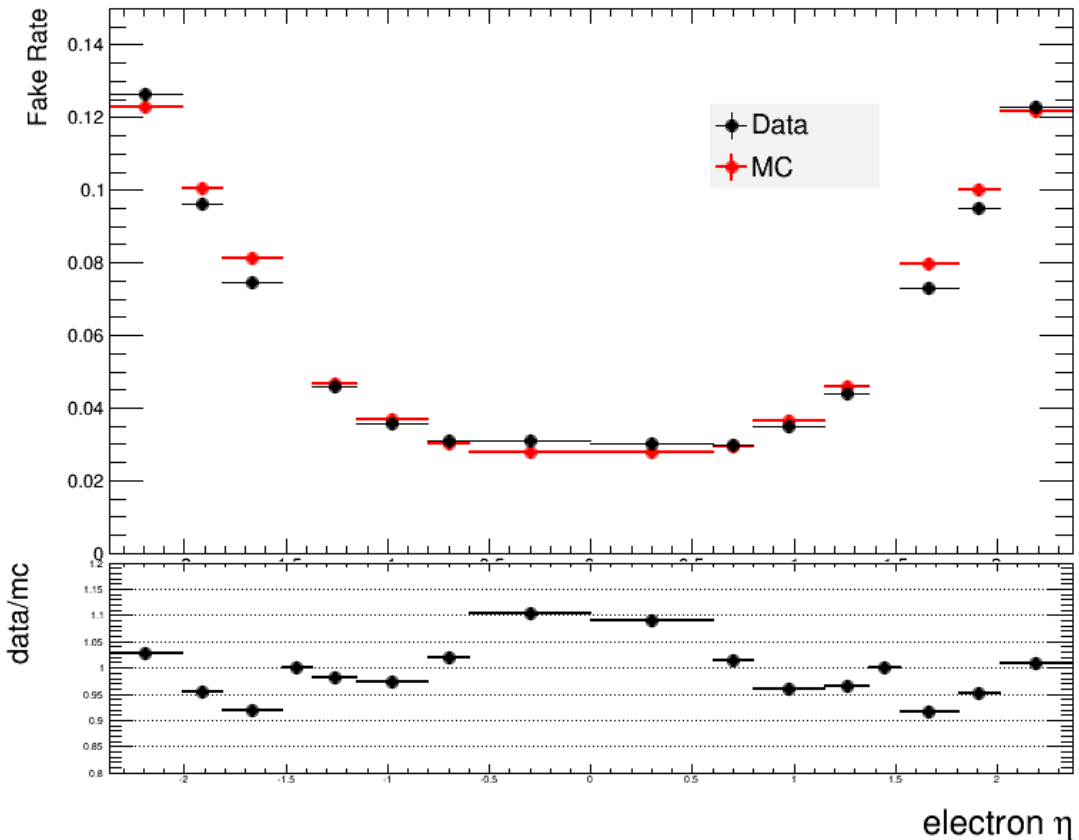


Figure 26: Comparison of the electron to photon fake rate measured for electrons reconstructed as photons using the 2015 and 2016 data (black) with the fake rate measured predicted by $Z \rightarrow ee$ Monte Carlo sample(red) vs η region from -2.37 to 2.37.

257 **7 Conclusion**

258 The electron-to-photon fake rate, defined as probability for a prompt electron to be reconstructed and
 259 selected as an isolated, tightly identified photon candidate divided by the probability for a prompt electron
 260 to be reconstructed and selected as an isolated, tightly identified electron candidate, which is simulated
 261 as the ratio of ambiguous electrons and photons originated from truth photon and all the truth electrons

262 with the full pp collision dataset collected at $\sqrt{s} = 13$ TeV in 2015 and 2016 by the ATLAS detector using
263 electrons from $Z \rightarrow ee$ samples. The fake rates range from 2.5% to 12.5% measured as a function of
264 pseudorapidity.

[Not reviewed, for internal circulation only]

²⁶⁵ The supporting notes for the analysis should also contain a list of contributors. This information should
²⁶⁶ usually be included in `mydocument-metadata.tex`. The list should be printed either here or before the
²⁶⁷ Table of Contents.

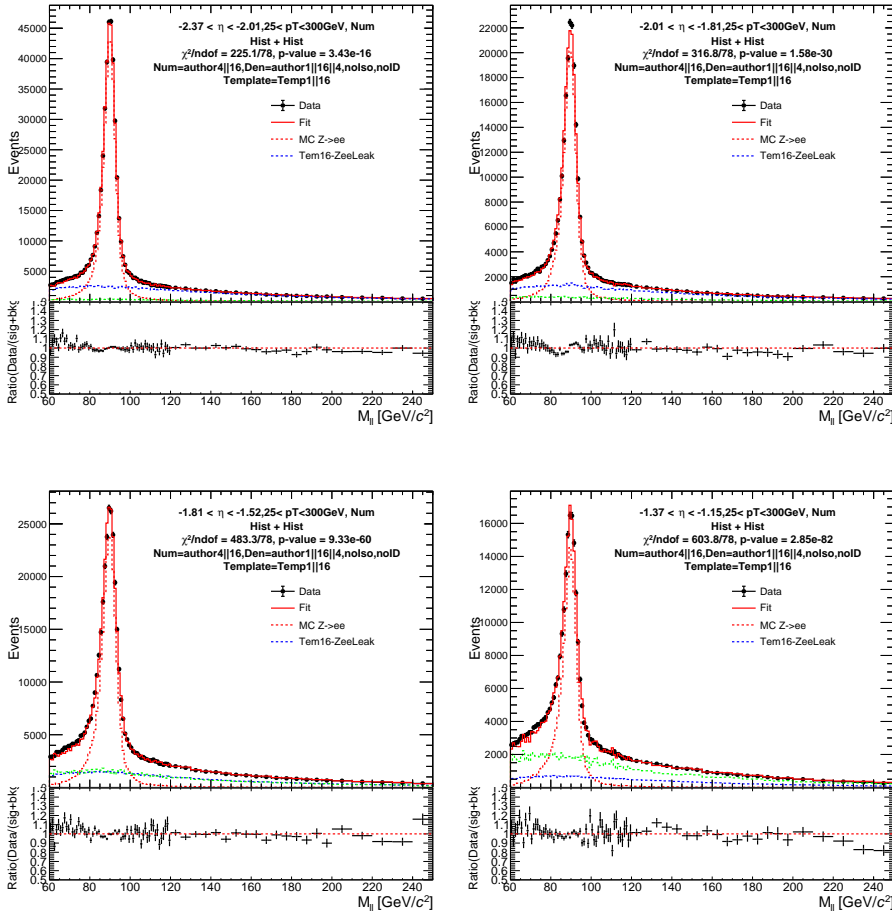
[Not reviewed, for internal circulation only]

²⁶⁸ **List of contributions**

²⁶⁹

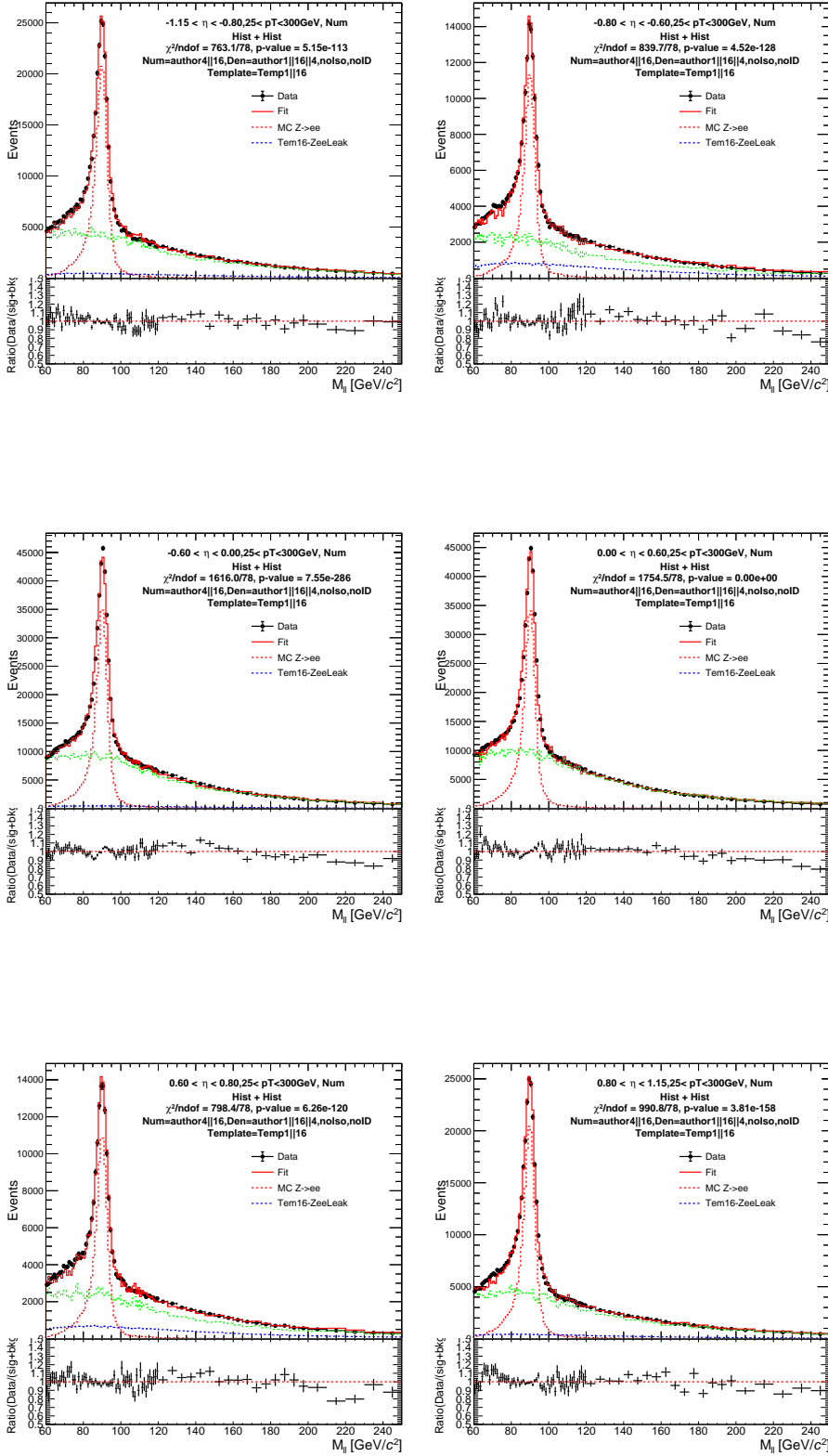
270 Appendices

271 A Fit results performance

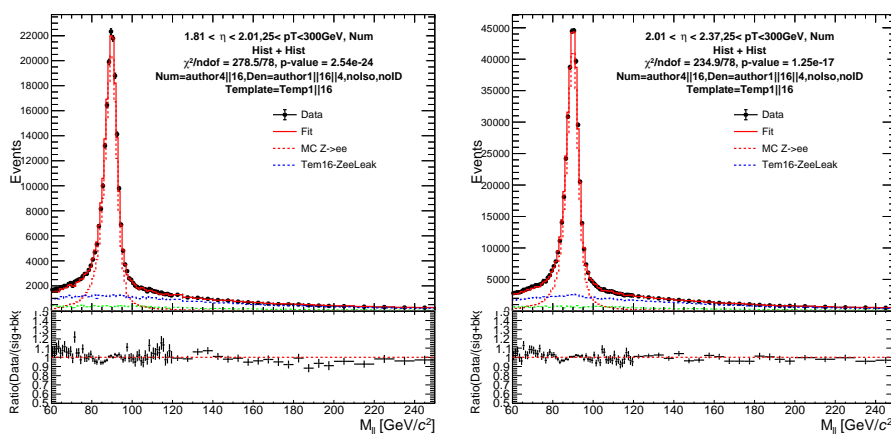
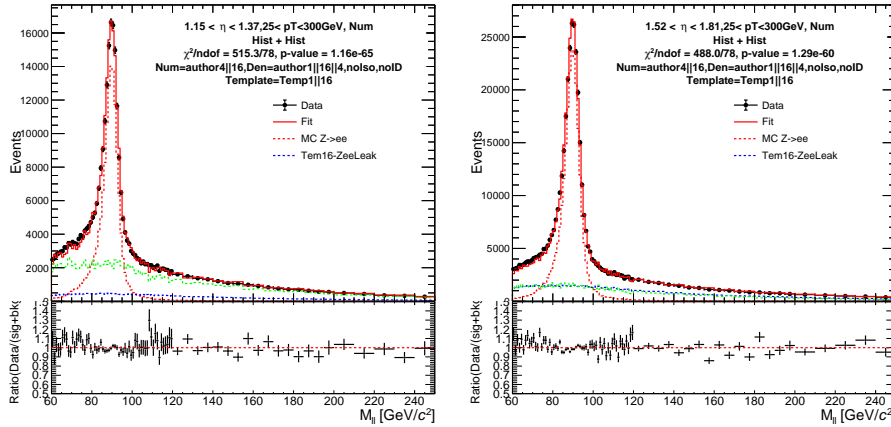


Not reviewed, for internal circulation only

Not reviewed, for internal circulation only



Not reviewed, for internal circulation only



272 In an ATLAS note, use the appendices to include all the technical details of your work that are relevant
273 for the ATLAS Collaboration only (e.g. dataset details, software release used). This information should
274 be printed after the Bibliography.

Not reviewed, for internal circulation only

275 References

- 276 [1] S. Frixione et al.,
277 *Matching NLO QCD computations with Parton Shower simulations: the POWHEG method*,
278 *JHEP* **0711** (2007) 070, arXiv: [1002.2581 \[hep-ph\]](#).
- 279 [2] T. Sjöstrand, S. Mrenna and P. Skands, *A Brief Introduction to PYTHIA 8.1*,
280 *Comput. Phys. Commun.* **178** (2008) 852, arXiv: [0710.3820 \[hep-ph\]](#).
- 281 [3] ATLAS Collaboration, *The ATLAS Simulation Infrastructure*, *Eur. Phys. J. C* **70** (2010) 823,
282 arXiv: [1005.4568 \[physics.ins-det\]](#).
- 283 [4] S. Agostinelli et al., *GEANT4: A simulation toolkit*, *Nucl. Instrum. Meth.* **A506** (2003) 250.